Climate adjustments over Africa accompanying the Indian monsoon onset

Pierre Camberlin, Bernard Fontaine, Samuel Louvet, Pascal Oettli, Patrick Valimba

Climate Adjustments over Africa Accompanying the Indian Monsoon Onset

P. CAMBERLIN AND B. FONTAINE

Centre de Recherches de Climatologie, UMR 5210 CNRS/uB, Université de Bourgogne, Dijon, France

S. LOUVET

HydroSciences Montpellier, UMR 5569, IRD/Université de Montpellier 2, Montpellier, France

P. OETTLI

Centre de Recherches de Climatologie, UMR 5210 CNRS/uB, Université de Bourgogne, Dijon, and LOCEAN, UMR 7159 NRS/IRD/UPMC/MNHN, Université Pierre et Marie Curie, Paris, France

P. VALIMBA

Department of Water Resources Engineering, College of Engineering and Technology, University of Dar es Salaam, Dar es Salaam, Tanzania

(Manuscript received 19 June 2009, in final form 18 November 2009)

ABSTRACT

Rainfall and circulation changes accompanying the Indian monsoon onset are examined, focusing on the African continent and neighboring areas. The Indian Meteorological Department official monsoon onset dates over Kerala (MOK; on average on 1 June) are used. Composites are formed at a pentad (5 days) time scale to compare pre- and postonset conditions. Climate Prediction Center (CPC) Merged Analysis of Precipitation (CMAP) data for 1979–2007 indicate that a substantial rainfall decrease over several parts of Africa is associated with MOK. Significant rainfall anomalies, after removal of the mean seasonal cycle, are found in eastern Africa and the nearby western Indian Ocean. Indian monsoon onset dates over the period 1958–2001 are correlated at 0.55 with the cessation dates of the March–May rainy season (the long rains) averaged over Kenya and northern Tanzania. The rainy season cessation leads the onset by 12 days, on average. An early cessation of the March–May rains tends to precede an early onset over India. Over East Africa, the rainfall decrease is associated with a strengthening of the southerly winds (Somali jet) shortly before MOK, enhancing wind divergence and wind shear.

A weaker rainfall signal is noted over western Africa and the Gulf of Guinea. MOK coincides with a pause in the progression of the West African monsoon. The pause is associated with anomalous descent over the Sahel, culminating two to three pentads after MOK. Composite maps further indicate that MOK is followed over much of the African continent by a sea level pressure rise and, between India and North Africa, a westward propagation of easterly wind and positive geopotential height anomalies. Many of these signals are associated with Madden–Julian oscillations, but independent features, suggesting Rossby wave propagation over North Africa, are also found to connect MOK and West Africa. Overall, these results are indicative of a large-scale adjustment of the atmospheric dynamics across both eastern and western Africa in conjunction with the monsoon onset over India.

1. Introduction

The onset of the Indian summer monsoon is a key step in the season unfolding, which sees the winter dry season being replaced by heavy rainfall over South Asia. It is also a much awaited event for rural communities from the Indian Subcontinent. The monsoon onset over Kerala, at the southern tip of India, heralds the progress of the monsoon rain belt over the rest of the country. It is closely monitored, and numerous studies have focused on the circulation changes associated with it, and the possibility to predict it. The monsoon onset over Kerala, which takes place on 1 June (for the period of 1911–2007), on average, actually accompanies large-scale, relatively abrupt circulation changes across the northern Indian Ocean and

Corresponding author address: Pierre Camberlin, 6 Bd Gabriel, Centre de Recherches de Climatologie, UMR 5210 CNRS/uB, Université de Bourgogne, 21000 Dijon, France.
E-mail: camber@u-bourgogne.fr

DOI: 10.1175/2009JCLI3302.1

Asia. Yin (1949) noted that the monsoon onset is related to the shift of the subtropical jet stream to the north of the Himalaya Mountains, which is then replaced by the tropical easterly jet (Koteswaram 1958). The importance of the Tibetan elevated heat source as a trigger to the monsoon onset was stressed by several authors (e.g., Flohn 1957; He et al. 1987; Murakami 1987; Li and Yanai 1996). Joseph et al. (1994) found increasing convection from the south Arabian Sea to South China and suppressed convection elsewhere, especially over the western Pacific at the time of the monsoon onset in southern India. These changes coincide with the establishment of strong low-level southwesterlies and the strengthening and expansion of upper-level easterlies. Interannual variations of onset dates were studied by Anantakrishnan and Soman (1988), Joseph et al. (1994), Raju et al. (2007), and Pai and Nair (2009), among others. Joseph et al. (1994) noted that late onsets were related to warm anomalies over the Indian and Pacific Oceans south of the equator (generally linked to El Niño), and cold anomalies in the tropical and subtropical oceans to the north. Based on a thermodynamic index of the Indian summer monsoon, Xavier et al. (2007) demonstrated that onset delay was due to adiabatic subsidence, which inhibits the vertical mixing of heat.

Given the scale of the atmospheric rearrangement, which coincides with the Indian monsoon onset, we may expect significant signals to be found away from South Asia and the northern Indian Ocean. The Indian summer monsoon flow takes the form of a low-level jet crossing the equator in East Africa, the so-called Findlater jet or Somali jet (Findlater 1969, 1978). Cadet and Desbois (1980) noted that the sudden establishment of the Somali jet along the East African coast precedes the first rainfall over the western coast of India by a few days. Recently, Boos and Emanuel (2009) found that an abrupt onset of the jet occurs over the Indian Ocean about 1000 km east of the East African highlands. The Indian monsoon also connects with the African monsoon by means of the southwesterlies originating from the South Atlantic Ocean and the nearby Congo basin, which reach Sudan and Ethiopia, and then converge with the Somali jet east of the Gulf of Aden. In the upper troposphere, the tropical easterly jet, which forms as a result of elevated heating over Tibet and latent heat release over South Asia, flows westward across Ethiopia and the Sudano–Sahelian belt. Joseph et al. (1994) presented outgoing longwave radiation (OLR) maps for pentads before and after the monsoon onset over Kerala. Changes over Africa were not discussed, although their maps indicate declining convection across central Africa from the onset pentad. Zorita and Tilya (2002) found a negative correlation between May rainfall in northern Tanzania and all-India summer monsoon rainfall. However, they did not consider the relationship with the monsoon onset.

Over the African continent, cases of abrupt rainfall transitions have been described by Riddle and Cook (2008) for the greater Horn of Africa region. Two jumps were documented: the first one occurs between late March and early April, when the rainfall belt moves above the equator, and the second one occurs in late May when rainfall decreases in equatorial East Africa and eastern Ethiopia and increases in western Ethiopia. The period between the two jumps coincides with the Somali jet being limited to a meridional branch over eastern Africa. After the second jump, the Somali jet is found to be fully formed. However, detailed relationships between these jumps and the onset of the Indian monsoon were not documented. Monsoon jumps have also been described in West Africa (Sultan and Janicot 2000, 2003; Le Barbé et al. 2002; Hagos and Cook 2007). Observations show an abrupt shift of the intertropical convergence zone (ITCZ) from the Guinean region around 5°N to the Sudanian region around 10°N in late June, but its mechanism is still unclear (Janicot 2009). Connections between intraseasonal variations of convection in the Indian and West African monsoon regions have been documented (Janicot et al. 2009), though with no particular focus on the onset.

In this study, we analyze the sequence of events, over the whole of tropical Africa, which coincides with the onset of the monsoon over southern India. It is hypothesized that a large-scale rearrangement in convective activity and atmospheric circulation over several parts of Africa is associated with the onset. To separate atmospheric changes truly associated with the Indian monsoon onset from mere coincidences in the annual cycle, both raw data and anomalies from the mean annual cycle, taking into account the interannual variations of the onset, were considered. It is still unknown, in particular, whether the jumps in the rainfall belt found in both eastern and western Africa in late May and June, respectively, bear any relationship with variations in the date of the Indian monsoon onset. These are important issues because any shift in the phasing of the rainy seasons (i.e., their onset and cessation), in both regions, affect crop growth.

Section 2 presents the three types of data used in the study, as well as the methods. The results are divided into three sections. Changes in the rainfall field at the time of monsoon onset are first considered (section 3), and then the atmospheric circulation is examined (section 4). We later focus on East Africa, where strong seasonal changes occur in conjunction with those of the Indian monsoon system (section 5).

2. Data and methods

a. Indian monsoon onset

The onset date of the monsoon used in this study is the official date published by the Indian Meteorological Department (IMD) for Kerala, at the southern tip of India (Joseph et al. 1994; Pai and Nair 2009). Though the IMD monsoon onset over Kerala (MOK) can by no means be considered as representative of the onset over all parts of India, it is acknowledged that it is not merely a local signal, but reflects large-scale circulation changes over the Indian Subcontinent and adjoining seas. A delay in the MOK is generally associated with a delay in onset at least over the southern and western states of India (Pai and Nair 2009).

The MOK is determined subjectively by IMD as a sustained increase in rainfall at the observation stations in Kerala and nearby islands, accompanying wind and humidity changes in the lower troposphere. Alternative definitions of the Indian monsoon onset have been discussed by Anantakrishnan and Soman (1988), Joseph et al. (1994), Xavier et al. (2007), Fasullo and Webster (2003), and Wang et al. (2009). Fasullo and Webster (2003) noted that the IMD onset masks some large-scale teleconnections, such as El Niño–Southern Oscillation (ENSO). Consequently, they used vertically integrated moisture transport over the Arabian Sea to identify the onset. Other objective methods are based on either several atmospheric parameters around Kerala (Joseph et al. 2006) or 850-hPa zonal wind only (Wang et al. 2009). As noted by Fasullo and Webster (2003) and Wang et al. (2009), there is still fair consistency between the dates given by the different authors and those from IMD, though in occasional years the difference exceeds 10 days. Over the period of 1971–2003, Joseph et al. (2006) obtained a correlation of 0.80 between their objectively defined onset dates and those from IMD, with a difference of no more than 5 days in 25 out of the 33 years analyzed. The IMD recently revised its criteria used to define MOK, by incorporating outgoing longwave radiation as well as wind data, in addition to rainfall (Pai and Nair 2009). In the present study, except for 2004–07, we retain the IMD dates based on the old criteria, because they are available over a longer period and have been used in most previous studies, which makes comparison with the present results more straightforward. For the largest part of the record period, the agreement between the IMD dates and other definitions is also very good (see Joseph et al. 2006, for a thorough comparison). The results below confirm that the traditional MOK is associated with large-scale circulation changes and not local-scale anomalies.

b. Rainfall data

Large-scale patterns of rainfall variations are assessed at a pentad (5 day) time scale using the Climate Prediction Center (CPC) Merged Analysis of Precipitation (CMAP) dataset (Xie and Arkin 1997). It covers the period of 1979–2007, at a 2.5° latitude × 2.5° longitude resolution. The area comprising most of the African continent, the western and central parts of the Indian Ocean, and southwestern Asia (35°S–35°N, 20°W–110°E) have been extracted. The version of the CMAP dataset used in this study incorporates only rain gauge and satellite estimates; no model outputs are used. It was shown that over continents the CMAP dataset has similar performance as other global gridded datasets (Yin et al. 2004). Composite analyses as depicted below using data from the Global Precipitation Climatology Project (GPCP) yielded similar results as those for CMAP.

For East Africa (Kenya and northeast Tanzania), daily rainfall data for 34 rain gauges were considered. The data mainly originate from the Kenya and Tanzania Meteorological Services and cover the period of 1958–87 (Camberlin and Okoola 2003, hereafter CAM). Some of the station time series have been updated to 2001. Quality control has been performed on the original data, based on a comparison of the monthly totals with an independent monthly rainfall dataset. Months showing discrepancies between the daily and the monthly data have been set as missing, and stations with more than 3 yr of missing data have been excluded, resulting in the final selection of the 34 stations.

c. Reanalysis data

Data depicting atmospheric conditions are taken from the National Centers for Environmental Prediction (NCEP)/Department of Energy (DOE) Global Reanalysis 2 (NCEP-2; Kanamitsu et al. 2002). Daily averages are available for the period of 1979–2007. The variables retained in the analysis are the meridional (V) and zonal (U) components of the wind at various pressure levels, surface temperature, sea level pressure, and midtropospheric (500 hPa) vertical velocity (W500). A regional index has been computed to describe the velocity of the cross-equatorial Somali jet over the western Indian Ocean (10°S–10°N, 40°–60°E), using the 850-hPa meridional flow. For comparison purposes, the same index has also been defined based on the 40-yr European Centre for Medium-Range Weather Forecasts (ECMWF) Re-Analysis (ERA-40) data (Uppala et al. 2005). A regional index has also been computed to depict mean horizontal wind divergence over East Africa (5°S–5°N, 35°–45°E).

The representation of the East African highlands is biased on reanalysis data. In the NCEP-2 data they

culminate at 1449 m over Kenya and 1974 m over Ethiopia, with a potential impact on the reproduction of the Somali jet. However, because the analyses focus on its temporal variability, they should not be impacted too much.

d. Methods

For the detection of the climate patterns that accompany the monsoon onset, composite analyses have been performed at various time scales. For daily analyses, the date of MOK is considered as day 0 and mean composites of both raw and deseasonalized (either centered or standardized) values for each day before and after MOK are computed. Averages over several consecutive days before and after the onset are also considered in order to better show the spatial patterns of the shift and to remove the noise associated with individual weather events. For pentad analyses, such as those carried out on CMAP rainfall data, pentad 0 (P0) is considered as the one in which MOK occurs, and composite means are similarly computed for pentads P-1, P-2, P-3, etc. before the onset (preonset), and P1, P2, P3, etc., after the onset (postonset). The Student's *t* test is used when working on anomalies to test whether the mean composite anomaly departs significantly from the long-term mean. As in Lawrence and Webster (2002), the reference annual cycle (for both the mean and the standard deviation) used for computing rainfall anomalies is the sum of the first three Fourier harmonics.

3. Large-scale rainfall changes

Rainfall fields are first considered to assess the changes accompanying the Indian monsoon onset over Kerala. Figure 1a shows the mean rainfall field at the time of the onset for reference. Heavy rainfall is found over the Arabian Sea and Bay of Bengal. The rains associated with the African monsoon are also found along the ITCZ between the equator and 10°N. A discontinuity is noted in eastern Africa (Somalia and neighboring areas). The change between preonset and postonset is shown in Figs. 1b,c, in millimeters and standardized anomalies, respectively. Preonset is considered as the average of P-2 and P-1 pentads, and postonset is the average of P1 and P2 pentads, following LinHo et al. (2008) who studied the patterns associated with the spring rains onset in South China.

As expected, the post-minus preonset maps display a large rainfall increase in the eastern Arabian Sea, the Bay of Bengal, and most of India. It is accompanied by a corresponding rainfall decrease over the southern Arabian Sea. Although the absolute variations are smaller, there are substantial changes over Africa as well. Rainfall decreases over East Africa (especially Somalia, Kenya, Uganda, and northern Tanzania) and the nearby Indian Ocean. A decrease is also found over the Gulf of Guinea, extending eastward inland up to Gabon. Slight rainfall increases are noted in the Sudanian belt, especially around Lake Chad and south of Senegal. However, in May and June, atmospheric conditions exhibit strong changes in much of the tropics, even if they are not impacted by the Indian monsoon onset. For instance, a major ITCZ shift occurs in western Africa in June (Sultan and Janicot 2000, 2003). Therefore, it is useful to consider both absolute rainfall variations and deseasonalized values. The pattern obtained for post-minus preonset pentads is not strongly different, however (Fig. 1c). Apart from the strong rainfall changes over southern Asia, the main signal is found over eastern Africa and the nearby Indian Ocean, where rainfall decreases significantly (Student's *t* test, with a 95% confidence level). There are also rainfall decreases over the equatorial Atlantic Ocean and increases over West Africa, which are restricted to small areas and are generally not significant. However, the change in East African rainfall, as found in the interannual anomalies, tends to show that the signal associated with the Indian monsoon onset is not purely local. Two pentads later (Fig. 2), the rainfall enhancement is still evident in the regions surrounding the Indian Subcontinent. The rainfall decrease found over eastern Africa and the nearby Indian Ocean persists, although it is almost insignificant. Over the Gulf of Guinea and parts of West Africa, rainfall anomalies show a relatively consistent decrease.

Regional rainfall averages over some key areas (boxed on Fig. 1a) have been computed, and the evolution of rainfall amounts before and after MOK is plotted on Fig. 3. The left panels display the raw values, and the right panels are the centered (dashed) and standardized (solid) anomalies with respect to the mean seasonal cycle. The MOK coincides with a strong rainfall decrease in the western Indian Ocean and East Africa (Kenya and Somalia). Negative anomalies exceed the 95% confidence level at P0 and P1 (stars, right panels, Fig. 3). It is noticeable that over Somalia (Fig. 3, left panel), the MOK pentad marks the start of a long, very dry sequence, corresponding to the boreal summer dry season. The strongest rainfall decrease is found between P-2 and P0 over Somalia and the western Indian Ocean. Over Kenya, the decrease is similar, though it tends to start earlier around P-3. The MOK thus seems to be associated with the onset of the boreal summer dry season over much of East Africa, a feature that is discussed in section 5. The fact that significant dry anomalies with respect to the seasonal cycle are found after MOK indicates that the relationship is not merely a covariation associated with the mean seasonal cycle. The relationship is preserved at interannual time

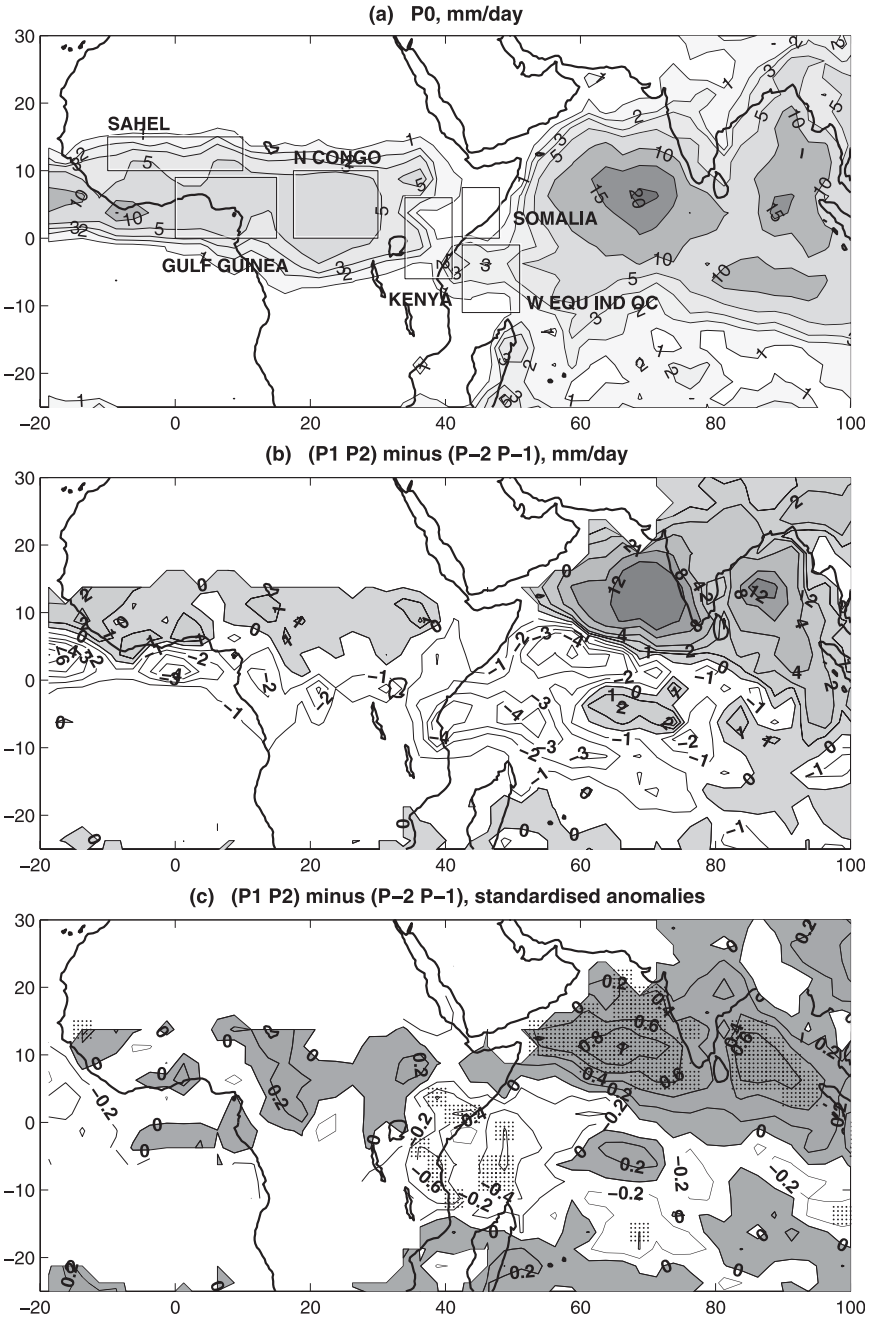

FIG. 1. (top) CMAP rainfall during the onset pentad of the Indian summer monsoon in Kerala (mm day^{-1}), and the difference (middle) between post- and preonset pentads (mm day^{-1}) and (bottom) in standardized anomalies. Positive anomalies in the bottom two panels are shaded; the significant (Student's *t* test, 95% confidence level) differences between the post- and the preonset pentads in the bottom panel are denoted (dotted areas). Boxes indicate the location of the rainfall indices used in Fig. 3.

scales, which makes us believe that the Indian monsoon onset has a dynamical connection with rainfall activity over East Africa.

Over the rest of Africa, the signal is not as consistent. Over the northern Congo basin, a statistically significant rainfall decrease also accompanies the monsoon onset in India at P1 (Fig. 3), although it is weak and not durable. Over the Gulf of Guinea, there is a small rainfall peak shortly before MOK, after which time a weak decrease is found toward P4; however, rainfall remains relatively

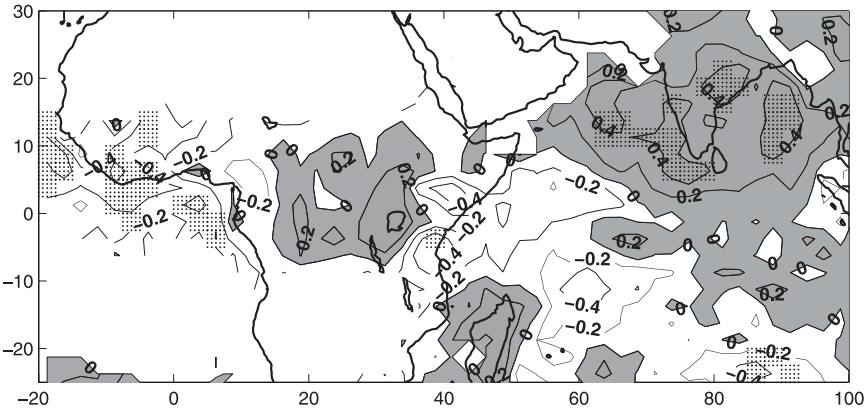

FIG. 2. Difference in CMAP standardized rainfall anomalies between post- and preonset pentads: pentads P3 and P4 minus pentads P-2 and P-1. Positive anomalies are shaded. Dotted areas denote significant (Student's *t* test, 95% confidence level) differences.

heavy over this region. The P4 negative anomaly is significant, but short lived. For the Sahel (Fig. 3, bottom panel), the marked rainfall increase found in the premonsoon season (from P-9 to P-3, and more significantly at P-2 and P-1) is interrupted from P0 to P4. The flat part of the plot (left panel) indicates that the seasonal rainfall does not increase any more, which translates in growing negative anomalies. The anomalies do not reach the 95% significance threshold, but the halt in the progress of the monsoon is clear. It partly coincides with the significant decrease in standardized rainfall anomalies found over much of West Africa between pentads P-2/P-1 and P3/P4 (Fig. 2). Sultan and Janicot (2000, 2003) and Fontaine et al. (2008) found a rainfall decrease over all of West Africa prior to the ITCZ shift over this region (on average, around 24 June). This decrease has also been presented as a pause in the northward shift of the monsoon rain belt (Louvet et al. 2003). The pause is consistent with the halt in the progress of the rainy season found between P0 and P4 (Fig. 3). A subsequent increase of rainfall activity is noted around P5, that is, around 25 June on average. This date is consistent with the above-noted ITCZ shift, and the associated monsoon onset over the Sahel (24 June; Fontaine and Louvet 2006).

These observations suggest that the MOK is associated with a decrease of rainfall activity over several parts of Africa, temporarily as in the Sahel or permanently as in East Africa. Over East Africa, the decrease starts some time before MOK. This observation is detailed in section 5. The fact that these decreases are found in both raw rainfall data and standardized anomalies suggests that it is a robust feature, and that the relationship with MOK is not a mere coincidence in the annual cycles. It has been verified (not shown) that the basic features of rainfall changes associated with MOK are found in both early and late-onset years. The use of alternative monsoon onset definitions also proved the robustness of the results. Using the objective definition for the onset over Kerala by Joseph et al. (2006), patterns very similar to those shown above for MOK were obtained. The same applies to the composites that were computed for the period of 1979–2000, based on the onset dates defined by Fasullo and Webster (2003), which use vertically integrated moisture transport over the Arabian Sea.

4. Large-scale circulation changes

The atmospheric dynamics associated with MOK are now examined. The sea level pressure (SLP) field at the time of the Indian monsoon onset (P0, see Fig. 4a) already shows a trough (below 1005 hPa) between the Arabian Peninsula and India. High pressure dominates the Southern Hemisphere subtropics. The change between pre- and postonset (Fig. 4b) is characterized by a fast SLP drop over the Gulf of Oman (up to 8 hPa in about 2 weeks). Weaker SLP increases occur over most of Africa, extending to the southwestern Indian Ocean and the South Atlantic Ocean. It should be noted that the boundary between negative and positive variations does not follow the meteorological equator, especially over western Africa where there is a general SLP increase, even close to the monsoon trough. In the southern subtropics, the pressure increase is strong over the South Atlantic and southern Africa, whereas a decrease is found in the southeastern Indian Ocean. This denotes a westward shift of the Mascarene high.

The low-level winds (shown for 850 hPa in Fig. 5a, with similar features for lower levels) display a strong cross-equatorial monsoon flow (Somali jet) in the western Indian Ocean at the time of MOK. This southerly flow curves again to the east, reaching the southern tip of India and the Myanmar coast. The southern Indian

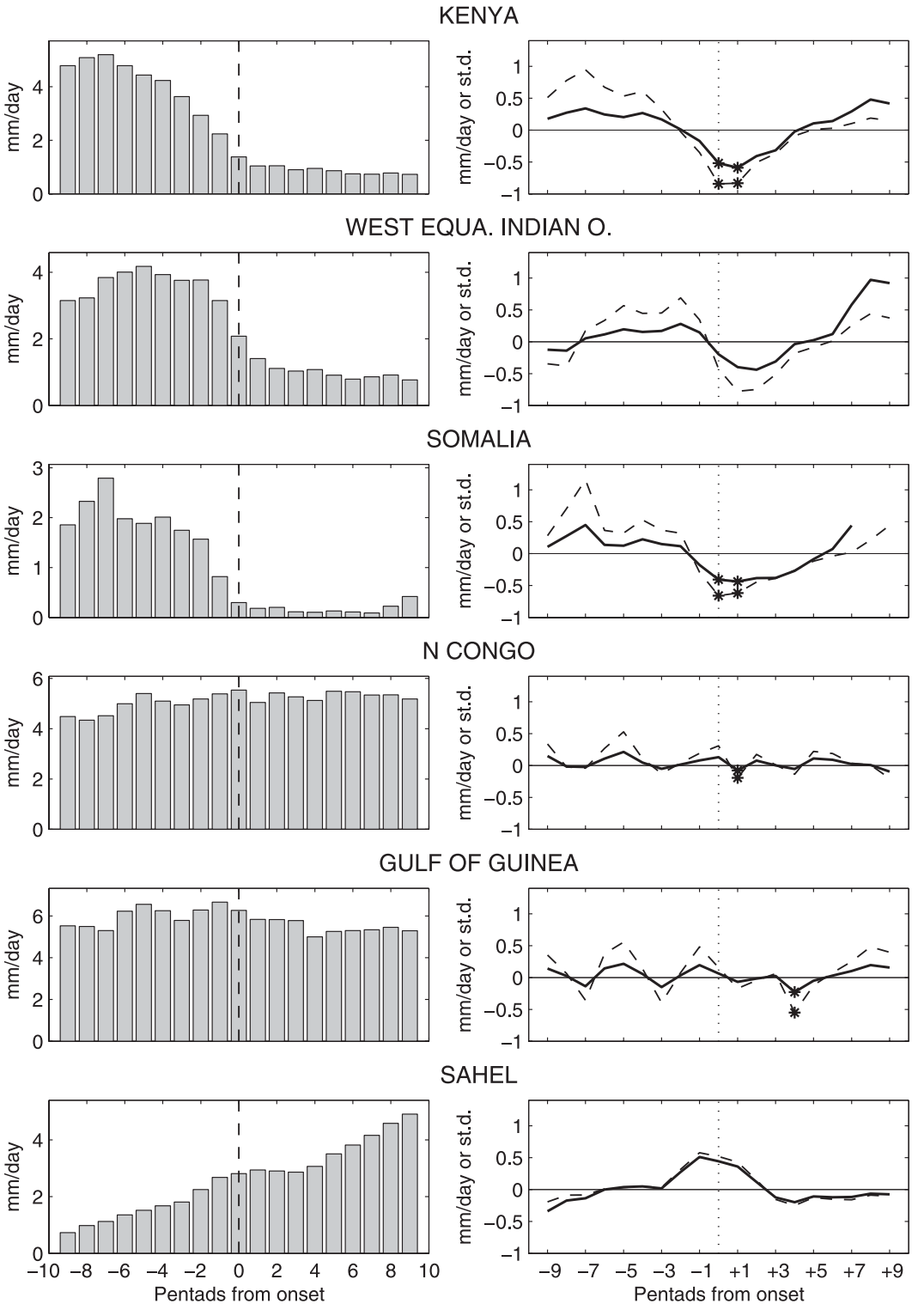

FIG. 3. Composite mean CMAP rainfall from nine pentads before to nine pentads after the MOK (pentad 0, dashed vertical line) over some regions of Africa and the neighboring oceans. (left) Raw values (mm day^{-1}) and (right) anomalies from the mean seasonal cycle, centered (dashed line, mm day^{-1}) and standardized (solid line). Stars indicate significant anomalies (Student's *t* test, 95% confidence level). Composite means have been smoothed using a three-point binomial filter.

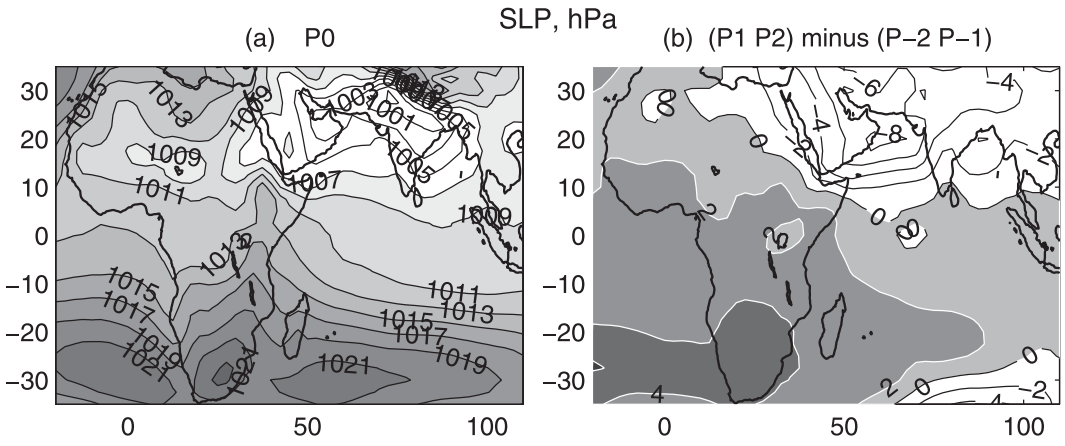

FIG. 4. (a) Sea level pressure (hPa) during the onset pentad of the Indian summer monsoon in Kerala, and (b) the difference between post- and preonset pentads. In (b), pressure rise is shaded.

Ocean easterlies, which feed the Somali jet, diverge over east-central Africa, with a branch toward the Gulf of Guinea. In the Sudano–Sahelian region, the southwesterly monsoon is still extremely shallow. The difference between the post- and preonset (Fig. 5a, right panel), as expected, indicates a considerable strengthening of the westerlies over the Arabian Sea and across India. This stronger westerly flow is related to anomalies in three different airstreams. The first airstream is from the southern Indian Ocean, with enhanced southerlies from the north of Madagascar. The second one is from the north, across the Red Sea area. There is also a third minor influx from the west, though the wind flow changes are restricted to the eastern Sahel, and do not span West Africa.

The upper troposphere (200 hPa, Fig. 5b) at the time of MOK displays the expected belt of easterlies over the northern Indian Ocean. It is sandwiched between the subtropical westerly jets. The Northern Hemisphere subtropical jet, at the longitude of Asia, has already shifted to the north, which is a characteristic feature of the atmospheric circulation changes that accompany the Indian monsoon onset (Yin 1949; Hahn and Manabe 1975; Rao et al. 2000; Raju et al. 2005). Only weak westerlies still affect Asia at latitudes of 25°–30°N. The difference between pre- and postonset pentads reveals considerable wind changes over most of the study area, including Africa. Easterly anomalies are ubiquitous. They are indicative of a general broadening of the upper easterlies in the Northern and Southern Hemispheres. Joseph et al. (1994) noted that at 150 hPa, the monsoon onset over Kerala coincides with a poleward shift of the subtropical jet streams in the two hemispheres at the longitude of India. Figure 5b also displays evidence of a northwestward extension of the tropical easterly jet after MOK.

In general, these patterns are suggestive of an enhancement of both the lateral (Hadley circulation between India and the southwestern Indian Ocean) and the transverse (east–west circulation between India and tropical North Africa) components of the monsoon, as depicted in Webster et al. (1998). Because simple difference maps may merely be a reflection of the mean seasonal cycle, standardized anomalies were computed as in section 3, enabling the identification of features specifically associated with MOK. For a better appraisal of the sequence of events, the anomalies were plotted as composite maps from two pentads before to four pentads after MOK. Figure 6 shows the results for the 850- and 200-hPa winds and geopotential heights (Z). At lower levels (850 hPa, see Fig. 6a), preonset pentads display northerly anomalies across the equatorial western Indian Ocean. They are associated with above-normal Z over the Arabian Peninsula and the northern Arabian Sea. At P0, a monsoon vortex anomaly quickly appears over the southern Arabian Sea. At the same time, positive Z anomalies tend to shift westward toward North and West Africa. The Indian monsoon trough deepens at P1, whereas Z further rises across most of the African continent. This results into the spreading of southerly wind anomalies from the western Indian Ocean to central Africa at P2. Note that there is a remarkable change from the preonset pentads, not only over the Arabian Sea, but also over most of tropical Africa south of the Sahara and the nearby South Atlantic Ocean, where Z850 strongly increases (Fig. 6a). However, low-level wind and geopotential height anomalies later on are weakening over much of the region (cf. P3 and P4) as the South Asian low shifts eastward to the Bay of Bengal then to South China.

At 200 hPa, the changes are even more striking (Fig. 6b). The westerly anomalies over the equatorial Indian Ocean at P-2 and P-1 disappear at P0. The onset pentad P0 is characterized by a burst of northerlies (near the equator)

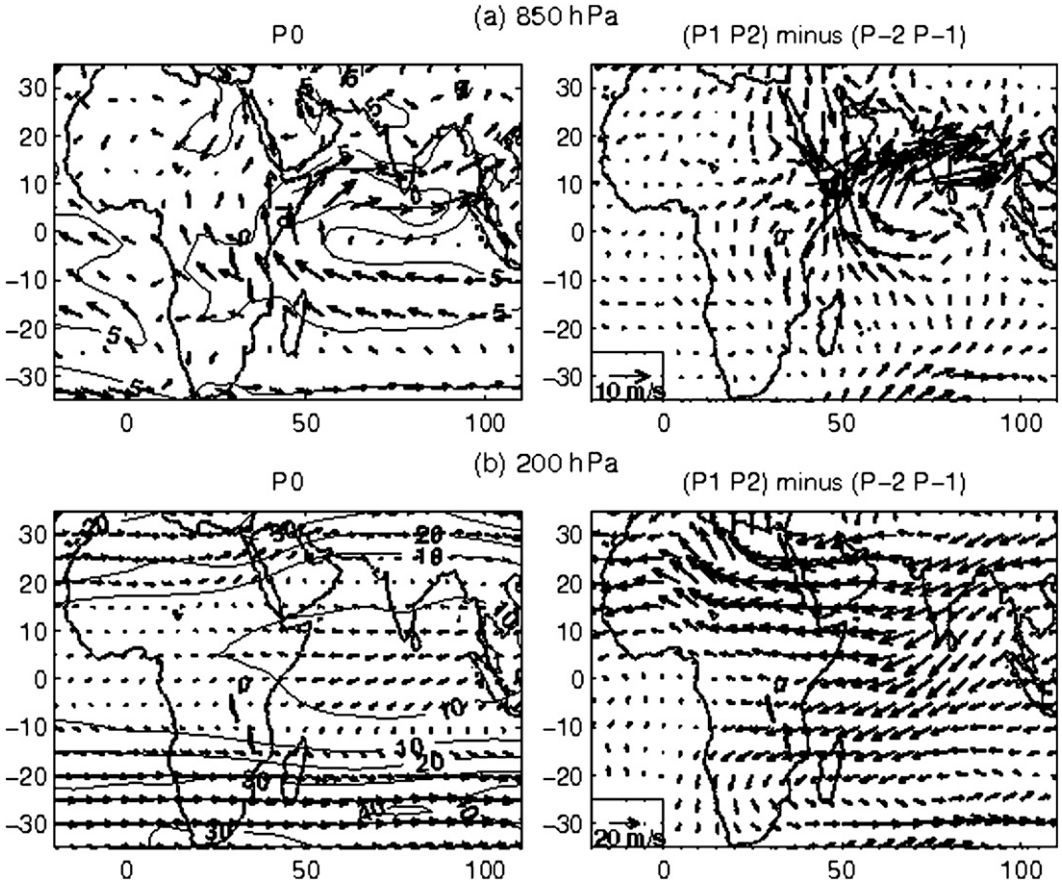

FIG. 5. (left) Wind flow during the onset pentad of the Indian summer monsoon in Kerala and (right) the difference between post- and preonset pentads. Units: m s^{-1}.

and southerlies (at latitudes of 20°–30°N) at the longitude of the Arabian Sea, that is, on each side of the convective area associated with the Indian monsoon onset. This is indicative of large-scale upper-tropospheric outflow, though the resulting mass increase starts only at P1, with twin anticyclonic gyres over the northern and southern Indian Ocean. The upper flow then organizes itself as a broad belt of anomalous easterlies. Note that the main flow is first directed mainly to the Southern Hemisphere (P1, lateral monsoon), then to the Northern Hemisphere via the tropical easterly jet (P2–P3, transverse monsoon). There is a westward strengthening of the anticyclonic anomaly from India toward the Arabian Peninsula and North Africa between P0 and P4 (Fig. 6b), while the corresponding Southern Hemisphere anticyclonic gyre fades away at P4. The westward propagation of easterly wind and geopotential height anomalies from the northern Arabian Sea to West Africa, along about 20°N, is even clearer in the midtroposphere (e.g., at 500 hPa, not shown). All circulation anomalies weaken at P5.

These results support a potential association between the Indian monsoon onset and weather activity over the African continent. For East Africa, the dynamical connection with the Indian monsoon is relatively straightforward. The enhanced low-level wind anomalies to the south of the Arabian Sea at the time of MOK are associated with divergence over East Africa. This point is further discussed in section 5. For West Africa, it is suggested that the upper-tropospheric changes that occur shortly after MOK are conducive to less favorable conditions over the region. Descent associated with the developing tropical easterly jet over Africa and the South Atlantic Ocean could explain the temporary negative rainfall anomalies found a few pentads after MOK, in particular, the pause in the West African monsoon as noted by Sultan and Janicot (2003) and Louvet et al. (2003). A composite of the 500-hPa vertical velocity over the Sahel region with respect to MOK (Fig. 7) shows a significant positive anomaly (anomalous descent) about 8–12 days (pentads P2–P3) after MOK. Rodwell and Hoskins (1996) noted a dramatic strengthening of descent over the eastern Sahara and the Mediterranean shortly after the onset of the Asian monsoon through Rossby wave propagation. The present results suggest that this

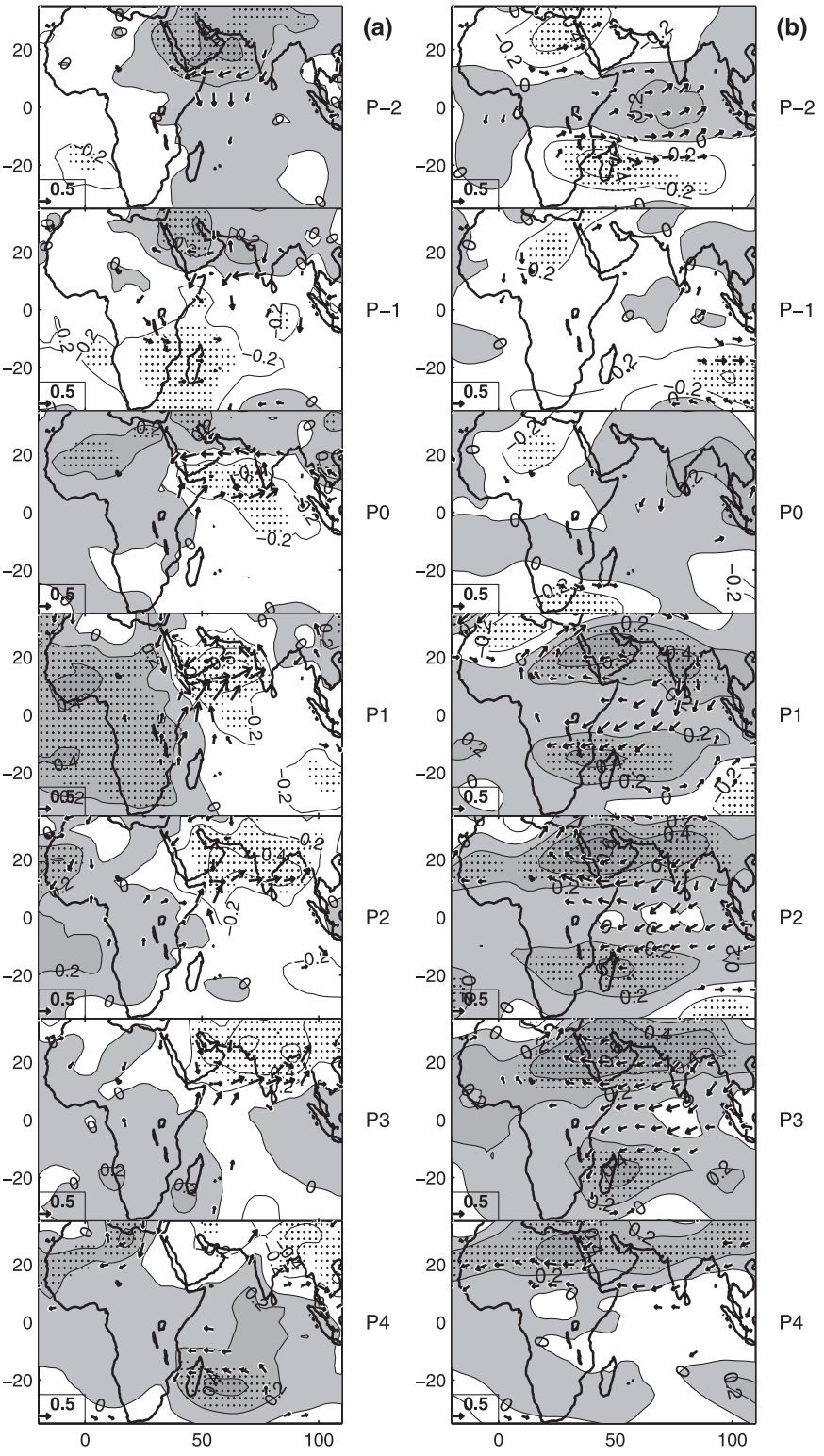

FIG. 6. Wind and geopotential height mean standardized anomalies for pentad P-2 to pentad P4 at (a) 850 and (b) 200 hPa. P0 is the Indian summer monsoon onset in Kerala. All values are in standard deviation units. Dots indicate significant geopotential heights anomalies (Student's *t* test, 95% confidence level). Only the wind anomalies significant at the 95% confidence level are shown as vectors.

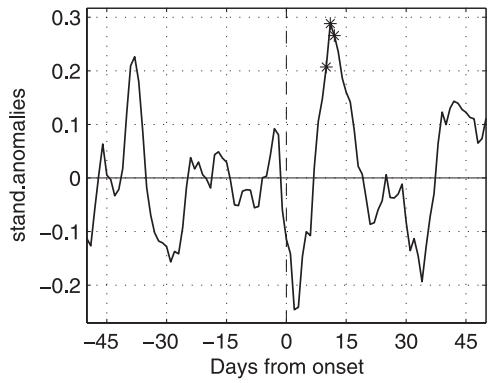

FIG. 7. Composite of 500-hPa vertical velocity standardized anomalies over the Sahel (10°–20°N, 20°W–20°E) from 50 days before to 50 days after the Indian monsoon onset over Kerala (dashed vertical line). Positive values denote descent anomalies. The series is smoothed using a 5-day moving average. Stars indicate significant anomalies (Student's *t* test, 95% confidence level).

mechanism also results in a weakening of rising motion in the monsoon regions of West Africa and a slight reduction in rainfall activity.

In general, the circulation patterns associated with MOK are strongly consistent with the anticipated response of the atmosphere to imposed heating, as portrayed by Gill (1980), for instance. The low-level flow to the west of India and along the eastern flank of Africa is close to the one associated with a combination of off-equatorial heating (asymmetrical about the equator; see Fig. 2 in Gill 1980) and equatorial heating (symmetrical; Fig. 1). The upper-tropospheric anticyclonic gyres in the two hemispheres, located to the west of the Indian longitudes and observed just after MOK, are more clearly associated with Gill's model of the response to a prescribed equatorial heating source. Note that these gyres are also strongly reminiscent of those associated with the Madden–Julian oscillation (MJO; Knutson and Weickmann 1987; Hendon and Salby 1994). Murakami et al. (1986) found that the installation and withdrawal of the South Asian summer monsoon is primarily determined by the phase changes of 25–90-day intraseasonal, MJO-type oscillations. The Indian monsoon onset over Kerala actually tends to occur when the enhanced convective phase of the MJO is located over the Indian Ocean (Wheeler and Hendon 2004). Weaker low-frequency intraseasonal oscillations (peaking around 40–50 days) have also been found in West Africa (Matthews 2004; Maloney and Shaman 2008; Pohl et al. 2009). The connections between MOK and rainfall and circulation anomalies over Africa may therefore partly reflect a response of both climate features to the MJO. Additional composite analyses (not shown) reveal that the rainfall and circulation anomalies found over West Africa in Figs. 3 and 6 are stronger when only the years in which MOK coincides with an MJO event in the Indian Ocean are used in the composite. This is particularly so for the rainfall decrease found over the Sahel and Gulf of Guinea after MOK. This decrease matches with the phase of reduced convection occurring over West Africa as the MJO-related convection shifts to the eastern Indian Ocean (Lavender and Matthews 2009; Pohl et al. 2009).

This demonstrates that the MJO plays a role in the Africa–MOK relationship. However, the patterns shown in the above composites do not fully reproduce those associated with the MJO. At the time of monsoon onset, the signal is dominated by cross-equatorial flows at both the lower and upper levels. There is also evidence of a westward shift of upper anticyclonic anomalies in the Northern Hemisphere only, which is not consistent with the dominantly eastward propagation of the MJO. Wu et al. (1999) actually noted that only in some years does the MJO show a strong contribution to the onset of the monsoon rains over India. Janicot et al. (2009) demonstrated that the active–break cycle of the Indian monsoon can influence the West African monsoon through a westward-propagating equatorial Rossby wave. Although part of the Rossby wave propagation from the Indian Ocean is related to the MJO (Matthews 2004; Lavender and Matthews 2009), Rossby wave activity may also develop outside MJO events. Figure 8 shows Hovmöller plots of 500-hPa geopotential height anomalies averaged over latitudes of 10°–30°N for pentads from P-2 to P4. This level is the one at which westward propagation over the region is most noticeable, but similar patterns are found at other tropospheric levels. The left panel corresponds to MOK events occurring within favorable phases of the MJO [phases 1–4 as in Wheeler and Hendon (2004), i.e., MJO convective activity over the Indian Ocean]. The right panel corresponds to the MOK events occurring at other phases. It is noisier because of a smaller sample: more onsets occur during MJO phases 1–4 than during phases 5–8. However, it is found that both composites exhibit a westward propagation of *Z* anomalies from India to North Africa, consistent with Rossby wave activity, with slight differences in their phase with respect to MOK and in their propagation speed. These results are in agreement with Janicot et al. (2009) for break and active phases of the Indian monsoon, and show a robust connection between the Indian monsoon onset and West African atmospheric dynamics, encompassing different time scales of variability. With the signal found over East Africa, this demonstrates that large-scale atmospheric adjustments occur over Africa in association with the Indian monsoon onset.

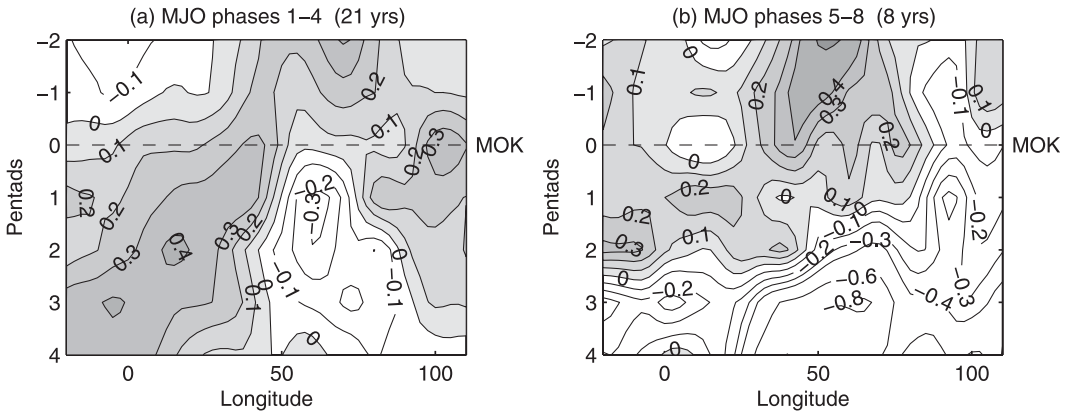

FIG. 8. Hovmöller diagram (time × longitude) of 500-hPa geopotential height standardized anomalies for pentad P-2 to pentad P4, averaged over latitudes of 10°–30°N. P0 is the Indian summer monsoon onset in Kerala. Positive values are shaded. Years for which MOK occurred during (a) phases 1–4 and (b) phases 5–8 of the MJO.

5. Relationships between MOK and East Africa climate

Given the significant changes found in rainfall and atmospheric dynamics over the eastern part of the African continent at the time of the Indian monsoon onset, a closer assessment of the sequence of events for this region is provided here. Another justification for this focus on East Africa is the complicated terrain, which, besides having a decisive influence on monsoon circulation (Krishnamurti et al. 1976, 1983; Hart 1977; Rodwell and Hoskins 1995; Slingo et al. 2004; Chakraborty et al. 2008), determines a number of different local climate regimes in the East African region itself (Ogallo 1985; Nicholson 1996).

In a previous study, CAM found some spatial coherence in the onset, and to a lesser extent the end of the March–May rainfall season (the long rains), in Kenya and northern Tanzania. The above results (Fig. 3) clearly show that MOK tends to coincide with the onset of the northern summer dry season in Somalia and Kenya. This aspect is further studied using a 30-yr (1958–87) daily rainfall dataset covering Kenya and northeast Tanzania, used in CAM. The data are treated as in CAM: a principal component analysis (PCA) is carried out on the square root–transformed daily time series for the period from February to June. The leading principal component (PC1) exhibits a relatively uniform signal across the region (not shown), with positive loadings everywhere, though with slightly higher loadings in a central corridor from Mount Kilimanjaro to northern Kenya. PC1 can therefore be considered as a representative regional index for daily rainfall in Kenya–northern Tanzania.

The corresponding PC1 scores are treated in a composite analysis similar to the ones carried out in section 3. Taking MOK as the reference date (day 0), composite scores from 50 days before day 0 to 12 days after have been computed (Fig. 9). It is confirmed that MOK occurs near the end of a period of very strong decrease in rainfall activity over Kenya and northern Tanzania (Fig. 9a). The drop in PC1 scores is acute between day −12 and day +3. This decrease follows a period of relatively sustained rainfall activity, shown as a flat interval around day −25 to day −15. These features are still apparent in the deseasonalized composite (Fig. 9b). A significant positive rainfall anomaly is found around day −14 to day −12, followed by a strong decrease leading to significant negative anomalies by day +2 to day +7. This further demonstrates that interannual variations of MOK are related to those of the late part of the East African long rains. The cyclical behavior of the composite anomalies, with a 30–40-day oscillation, suggests an involvement of the MJO.

The extent to which a significant rainfall decrease (greater than 0.5 standardized anomalies in 7 days) could herald monsoon onset has been tested by computing probabilities of onset for each day from the beginning of May. Figure 10 shows the probability of MOK occurrence within 5–10 days after each day of the sequence. A peak (solid line) is found around 20–25 May, that is, as expected, around 5–10 days before the average monsoon onset date (1 June). The same probability is then computed, but on the condition of a rainfall decrease in Kenya (dashed line in Fig. 10). It is shown that the conditional probability is greater compared to the raw one, especially between 20 and 30 May. For instance, about 80% of the rainfall decreases occurring around 22 May are followed by MOK 5–10 days afterward. The decrease of rainfall activity over East Africa, therefore, has some potential for the short-range prediction of MOK. The predictive potential of the long rains cessation to MOK onset has been further tested based on

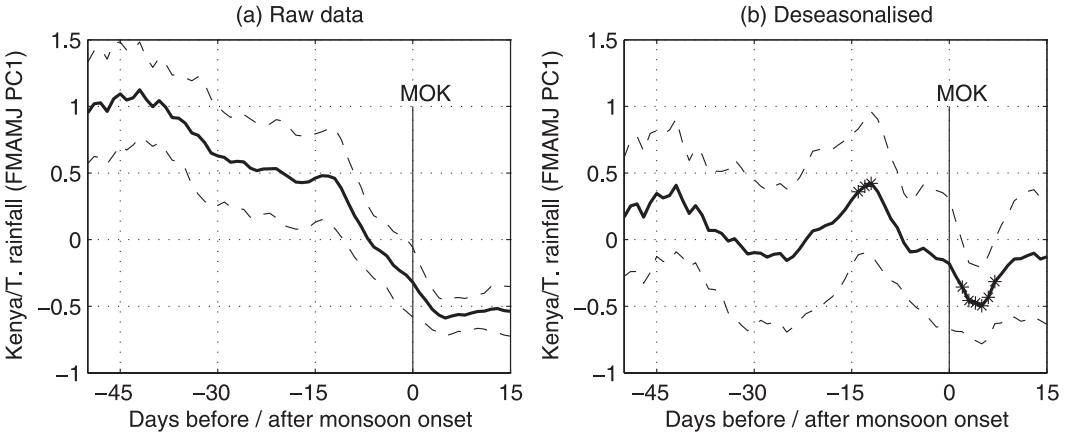

FIG. 9. Mean composite of the leading principal component of February–June daily rainfall over Kenya and northern Tanzania (PC1 scores), for 50 days before to 12 days after the onset of the Indian summer monsoon over Kerala (1958–87): (a) raw values and (b) deseasonalized anomalies. The time series have been smoothed using a five-point moving average. The upper (lower) envelopes show the mean plus (minus) 0.5 standard deviation. Stars in (b) denote significant anomalies (Student's *t* test, 95% confidence level).

a linear regression model, with a leave-one-out cross validation. The correlation coefficient between predicted and observed onset dates, in cross-validation mode, is 0.49, and the Brier skill score is 0.24. This positive score means that a MOK forecast based on the long rains cessation dates offers an improvement over the climatological forecast.

Because the rainfall decrease occurs near the end of the rainy season, the regional average of the long rains cessation dates in Kenya–northern Tanzania are next extracted, following the method presented in CAM. Using a smaller number of stations, the period of study is extended to 2001. PC1 of the daily rainfall is recomputed and the scores are analyzed for each year separately. The cessation date is the day that coincides with the peak in accumulated PC1 scores from 1 February, because a sustained decrease of the scores is associated with dry periods. It has been shown (CAM) that the dates obtained are representative of the local cessation dates in a large part of Kenya, although the long rains cessation is not as sharp as the onset, and it shows more discrepancies between subregions. On average, the East African long rains cessation takes place on 19 May, that is, 12 days before MOK (an average date of 31 May over the period of 1958–2001). The time series of the long rains cessation dates and MOK are displayed in Fig. 11. The correlation between the two time series (1958–2001) is 0.55, significant at the 99% confidence level. A late end of the long rains always coincides with a late onset of the monsoon. In 13 years in the period of 1958–2001, the long rains were prolonged after 25 May, with late MOK in all the 13 years (on average, by 7 days) except in 1966, when it was just average (31 May). An early end of the long rains also coincides with an early MOK, with some exceptions like that in 1997 where the long rains ended on 6 May but the monsoon onset over Kerala occurred on 9 June. Note that the definition of both the long rains cessation and the Indian monsoon onset are not unequivocal. For instance, in 1997 some rains continued to be recorded at several stations across the month of May.

Given these spatial discrepancies, a station-by-station analysis of East Africa rainfall was carried out. Standardized rainfall anomalies, with respect to the seasonal

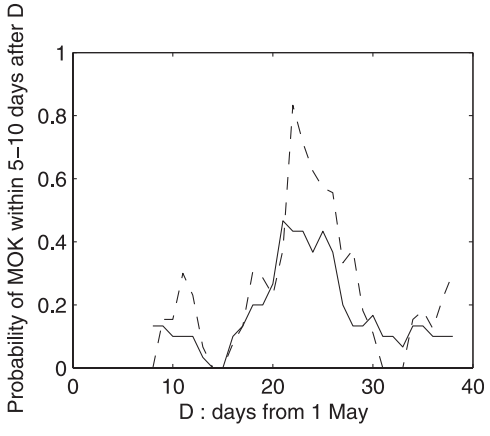

FIG. 10. Probability of monsoon onset over Kerala occurring within the 5–10 days following each day D from 1 May (solid line). The dashed line shows the same probability, on the condition that a significant rainfall decrease (less than −0.5) occurs in Kenya–northeastern Tanzania. The decrease is computed over a period of 7 days, ending on date D, using smoothed (5-day moving average) PC1 scores.

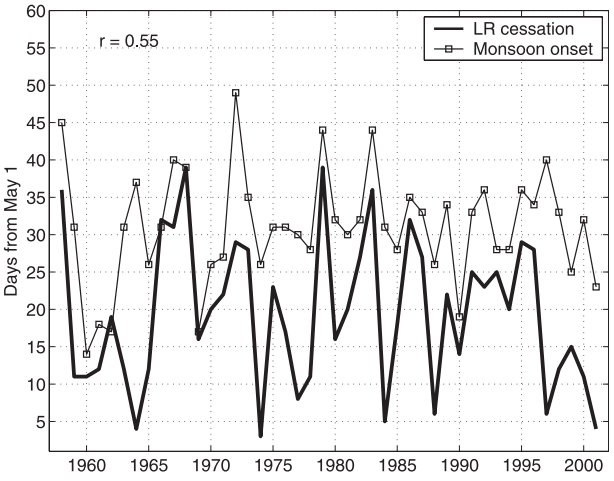

FIG. 11. Time series of the long rains cessation in Kenya–Tanzania and Indian monsoon onset over Kerala, 1958–2001.

cycle, are plotted as 5-day means from 17 days before to 8 days after MOK (Fig. 12). Dry conditions appear as early as 12 days before MOK in northeastern Kenya. They tend to spread to other stations 7 days before MOK, with the largest anomalies still in northeastern Kenya. In summer, this region is characterized by a strong diffluence of the southerly monsoon flow, which splits into the main low-level jet, running northeastward through Somalia, and the Turkana jet, running northwestward between the Kenya and Ethiopian highlands (Kinuthia and Asnani 1982). The early drying up in this region is suggested to indicate the setup of this circulation pattern. The rainfall composites (Fig. 12) also show that just after MOK dryness is enhanced, with negative anomalies becoming significant across southeastern Kenya, including the coast, and in Tanzania. Note that these dry conditions are preceded by a very wet spell around 12 days before MOK, which is consistent with the above findings on the cessation of the long rains. Stratification of the composites with respect to the MJO phases did not alter the results strongly, showing that the relationship between MOK and East Africa rainfall is a robust feature that cannot be only ascribed to a common response to the MJO.

Variations in the local wind associated with the monsoon onset are difficult to assess accurately given the resolution and quality of global-scale reanalysis products in a region with complex orography. Figure 13

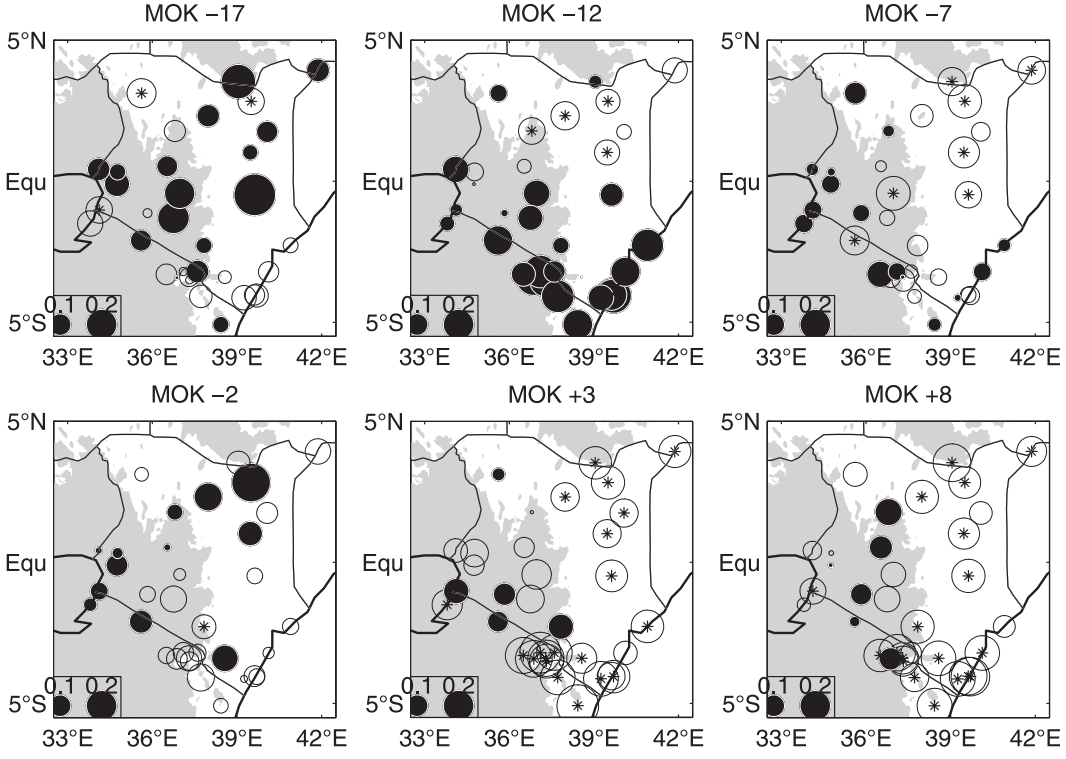

FIG. 12. Five-day mean standardized rainfall anomalies over Kenya and northeastern Tanzania from 17 days before (MOK −17) to 8 days after (MOK +8) the onset of the Indian monsoon. The day noted above each panel corresponds to the center of each 5-day period. Black (white) circles denote positive (negative) anomalies. The circle size is proportional to the anomaly (in standard deviation units). Stars indicate significant negative anomalies (Student's *t* test, 95% confidence level; positive anomalies are not significant). Shading shows areas above 1000 m.

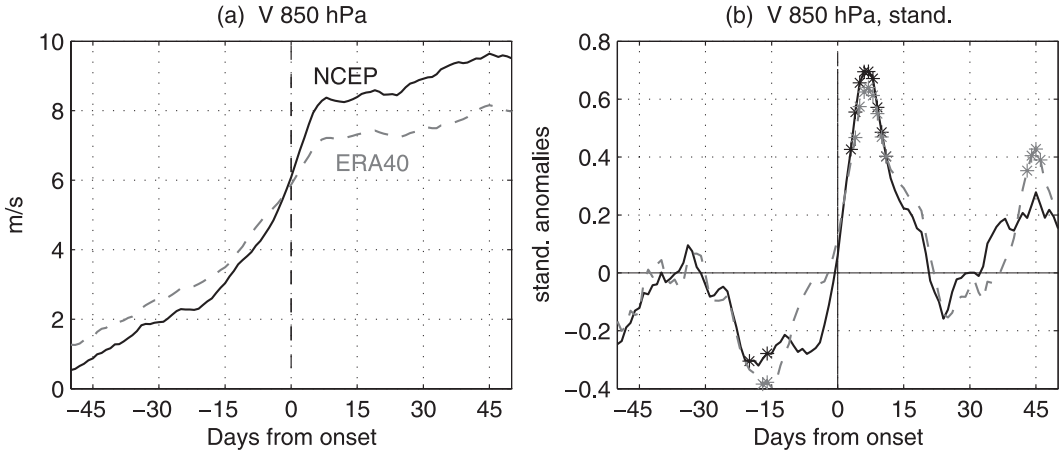

FIG. 13. Composites of the 850-hPa meridional wind flow over the western Indian Ocean–coastal East Africa region (10°S–10°N, 40°–60°E) from 50 days before to 50 days after the Indian monsoon onset over Kerala: (a) raw values and (b) deseasonalized values. The series are smoothed using a 5-point moving average. The black solid (gray dashed) lines refer to the NCEP-2 (ERA-40) data. Stars in (b) indicate significant anomalies (Student's t test, 95% confidence level).

displays a composite of the meridional wind flow in the western Indian Ocean–coastal East Africa region, with day 0 being the monsoon onset over Kerala. Given the paucity of radiosonde stations in the region, and to test the robustness of the signal, both NCEP-2 and ERA-40 were used to compute the wind flow index. A large increase in the southerly component of the wind at 850 hPa is found around MOK. Though the wind speed before (after) MOK tends to be higher (lower) for the ERA-40 index than for NCEP-2, the increase is noticeable in both datasets (Fig. 13, left panel). The deseasonalized anomalies (right panel) show that the meridional wind for both datasets is weaker than normal around day −15, and then strongly increases to reach positive, significant anomalies between days +3 and +12. The intensification of the wind tends to occur slightly earlier in ERA-40 than in NCEP-2. In both datasets, it precedes the actual onset, although the wind keeps on strengthening shortly after MOK. About a week after the onset, however, the speed increase comes to a halt and the Somali jet intensity remains quite steady thereafter (Fig. 13, left panel). There is also evidence of a 30–40-day oscillation, suggesting that part of the variations in the Somali jet intensity associated with MOK could be related to the MJO. The strong intensification of the jet at the time of Indian monsoon onset is similar to that found by Boos and Emanuel (2009), although their analysis revealed that the jet onset in the region adjacent to the East African highlands is not as rapid as farther east over the western Indian Ocean.

The strengthening of the Somali jet to the east of the East African highlands prior to and at the time of MOK (especially from days −15 to +5) would increase low-level wind divergence and horizontal/vertical wind shear over East Africa, which could explain the drying up in this region. To confirm this hypothesis, horizontal divergence was computed and averaged over an area covering Kenya and northern Tanzania (5°S–5°N, 35°–45°E). Composites indexed on MOK are plotted in Fig. 14. Although the divergence series are relatively noisy, there is a clear increase in local divergence at both 850 and 700 hPa some 10–15 days before MOK (left panels). Deseasonalized plots (right panels) show that the increase results in positive significant anomalies before and at the time of the monsoon onset over Kerala. This has a detrimental effect on convection over East Africa. The timing of the dynamical and rainfall anomalies are relatively consistent, with the drying up starting in northeastern Kenya about 7–12 days before MOK (Fig. 12), and then spreading to most of Kenya and northern Tanzania. Note that the Kenyan coast remains wet through to the date of monsoon onset over Kerala. Several authors have described wet spells along the East African coast, followed by a drying up accompanying a temporary strengthening of the Somali jet (Findlater 1974; Rodwell 1997), though coastal wet spells are more generally associated with easterly disturbances (Lumb 1966; Camberlin and Planchon 1997; Okoola et al. 2008).

These results indicate a phase locking between the long rains cessation over East Africa and the monsoon onset over India as a result of the dynamical link involving the low-level cross-equatorial flow (Somali jet). An India–East Africa connection was found by Zorita and Tilya (2002), who documented a negative correlation

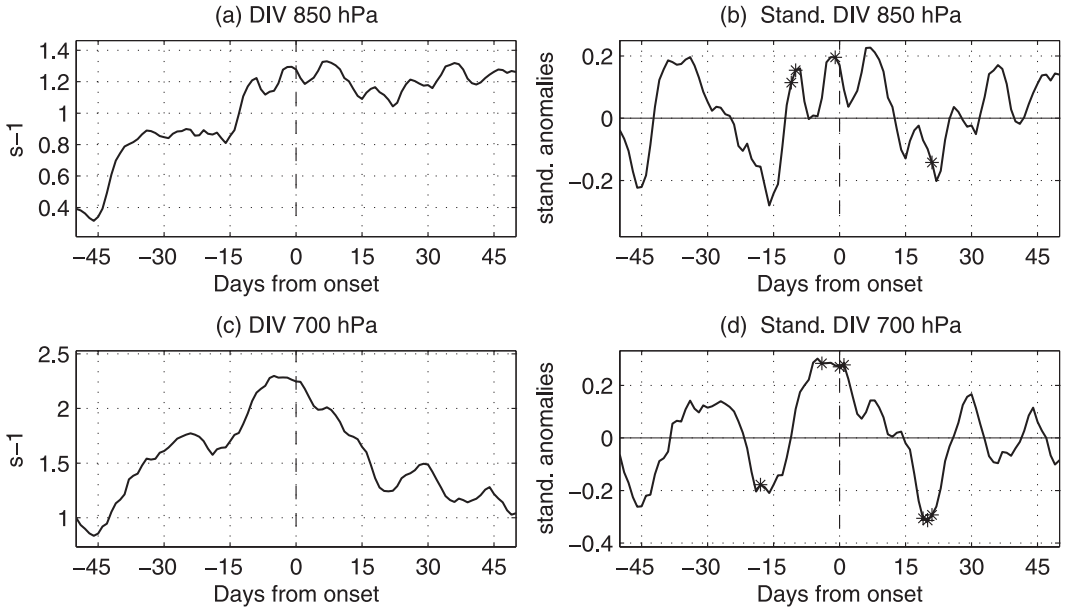

FIG. 14. NCEP-2 composites of horizontal wind divergence over Kenya–northern Tanzania (5°S–5°N, 35°–45°E) from 50 days before to 50 days after the Indian monsoon onset over Kerala: (left) raw values and (right) deseasonalized values (stars indicate anomalies significant at the 95% confidence level). The series are smoothed using a five-point moving average.

between May rainfall in northern Tanzania and all India summer monsoon rainfall. This means that lower-than-normal rainfall at the end of the long rains is followed by a ''good'' monsoon over India. Although this study did not consider the monsoon onset itself, it is consistent with the above results, which actually show that the relationship is related to the inverse phasing of the rainy seasons in the two regions.

6. Conclusions

The onset of the Indian monsoon is found to be accompanied by significant changes in atmospheric circulation and rainfall not only over South Asia but over parts of the African continent as well. Using the official IMD date of monsoon onset over Kerala as a reference, a decrease in rainfall activity is noted over several parts of Africa and the surrounding oceans at the time of the Indian monsoon onset. This decrease is still found in the interannual anomalies, after extraction of the mean annual cycle.

A particularly strong signal is found over East Africa. Marked decreases of rainfall activity at the end the March–May rainy season (the ''long rains'') over this region are indicative of a forthcoming onset of the monsoon over Kerala. Interannual time series of the long rains cessation dates over East Africa (Kenya and northeastern Tanzania) are significantly correlated (r = 0.55 for 1958–2001) with those of the Indian monsoon onset over Kerala. A late long rains cessation tends to precede a late monsoon onset. The rainfall decrease over East Africa (especially northeastern Kenya) is associated with the intensification of the Somali jet, which displays strong divergence over Kenya and Somalia and then flows toward India. Increased divergence is found before the Indian monsoon onset. There is some predictability potential in this relationship between India and East Africa because, on average, the cessation of the rains over East Africa leads the onset of the monsoon by 12 days, though the lead time varies from year to year.

Other parts of Africa (the Congo basin, Gulf of Guinea, and Sudano–Sahelian belt) also display reduced rainfall at the time of the Indian monsoon onset. However, the decrease is not as strong as in East Africa and tends to lag the onset. The Indian monsoon onset over Kerala coincides with a pause of about 15 days in the seasonal progression of rainfall over the Sudano–Sahelian region. The northward shift of the ITCZ over western Africa, which is associated with the rainy season onset over the Sahel, only occurs after this pause. Some rainfall reduction connected to the Indian monsoon onset over Kerala also occurs farther south over the Gulf of Guinea region.

These drier conditions are suggested to result from large-scale rearrangements in the zonal circulation between Asia and Africa. The convective burst associated with the Indian monsoon onset is related to an enhanced cross-equatorial flow and dryness installation over East

Africa (lateral monsoon), followed one to two pentads later by stronger upper-tropospheric easterlies (transverse monsoon). A pressure rise also occurs over much of Africa and the South Atlantic Ocean. Midtropospheric subsidence anomalies are found over the Sahel region 10–15 days after the onset. They may either be associated with the descending tropical easterly jet emanating from South Asia [enhancement of the transverse monsoon; see Webster et al. (1998)], or related to the strong subsidence generated over eastern Sahara and Mediterranean as a result of a Rossby wave propagation (Rodwell and Hoskins 1996; Janicot et al. 2009). The connection between Africa and India is also suggested to reflect a common imprint of the Madden–Julian oscillation, which is known to affect intraseasonal variations of the Indian monsoon, and has recently been shown to have some influence on the West African monsoon as well. Stratification of monsoon onsets according to the MJO phases shows that part of the rainfall reduction in West Africa after the onset results from the MJO. However, both the rainfall reduction in eastern Africa and the Rossby wave propagation across North Africa, associated with the monsoon onset, are still found outside ''favorable'' MJO phases. Though these aspects deserve further study, such findings support the hypothesis of large-scale rearrangements of the atmosphere over Africa in connection with Indian monsoon onset.

Acknowledgments. The authors wish to thank the Kenya and Tanzania Meteorological Departments for provision of part of the rainfall data used in the study. Very constructive comments from two anonymous reviewers are also gratefully acknowledged.

REFERENCES

Anantakrishnan, R., and M. K. Soman, 1988: The onset of the south-west monsoon over Kerala: 1901–1980. *J. Climatol.,* **8,** 283–296.

Boos, W. R., and K. A. Emanuel, 2009: Annual intensification of the Somali jet in a quasi-equilibrium framework: Observational composites. *Quart. J. Roy. Meteor. Soc.,* **135,** 319–335.

Cadet, D. L., and M. Desbois, 1980: The burst of the 1978 Indian summer monsoon as seen from METEOSAT. *Mon. Wea. Rev.,* **108,** 1697–1701.

Camberlin, P., and O. Planchon, 1997: Coastal precipitation regimes in Kenya. *Geogr. Ann.,* **79A,** 1–2, 109–119.

——, and R. E. Okoola, 2003: The onset and cessation of the ''long rains'' in eastern Africa and their interannual variability. *Theor. Appl. Climatol.,* **75,** 43–54.

Chakraborty, A., R. S. Nanjundiah, and J. Srinivasan, 2008: Impact of African orography and the Indian summer monsoon on the low-level Somali jet. *Int. J. Climatol.,* **29,** 983–992, doi:10.1002/joc.1720.

Fasullo, J., and P. J. Webster, 2003: A hydrological definition of Indian monsoon onset and withdrawal. *J. Climate,* **16,** 3200–3211.

Findlater, J., 1969: A major low-level air current near the Indian Ocean during the northern summer. *Quart. J. Roy. Meteor. Soc.,* **95,** 362–380.

——, 1974: The low-level cross-equatorial air current of the western Indian Ocean during the northern summer. *Weather,* **29,** 411–416.

——, 1978: Observational aspects of the low-level cross-equatorial jet stream. *Monsoon Dynamics,* T. N. Krishnamurti, Ed., Birkhäuser Verlag, 1251–1262.

Flohn, H., 1957: Large-scale aspects of the ''summer monsoon'' in south and East Asia. *J. Meteor. Soc. Japan,* **35,** 180–186.

Fontaine, B., and S. Louvet, 2006: Sudan-Sahel rainfall onset: Definition of an objective index, types of years, and experimental hindcasts. *J. Geophys. Res.,* **111,** D20103, doi:10.1029/2005JD007019.

——, ——, and P. Roucou, 2008: Definition and predictability of an OLR-based West African monsoon onset. *Int. J. Climatol.,* **28,** 1787–1798, doi:10.1002/joc.1674.

Gill, A. E., 1980: Some simple solutions for heat-induced tropical circulation. *Quart. J. Roy. Meteor. Soc.,* **106,** 447–462.

Hagos, S. M., and K. H. Cook, 2007: Dynamics of the West African monsoon jump. *J. Climate,* **20,** 5264–5284.

Hahn, D. G., and S. Manabe, 1975: The role of mountains in the South Asian monsoonal circulation. *J. Atmos. Sci.,* **32,** 1515–1541.

Hart, J. E., 1977: On the theory of the East African low level jet stream. *Pure Appl. Geophys.,* **115,** 1263–1282.

He, H., J. W. McGinnis, Z. Song, and M. Yanai, 1987: Onset of the Asian monsoon in 1979 and the effect of the Tibetan Plateau. *Mon. Wea. Rev.,* **115,** 1966–1995.

Hendon, H. H., and M. L. Salby, 1994: The life cycle of the Madden–Julian oscillation. *J. Atmos. Sci.,* **51,** 2225–2237.

Janicot, S., 2009: A comparison of Indian and African monsoon variability at different time scales. *C. R. Geosci.,* **351,** 575–590, doi:10.1016/j.crte.2009.02.002.

——, F. Mounier, N. M. J. Hall, S. Leroux, B. Sultan, and G. N. Kiladis, 2009: Dynamics of the West African monsoon. Part IV: Analysis of 25–90-day variability of convection and the role of the Indian monsoon. *J. Climate,* **22,** 1541–1565.

Joseph, P. V., J. K. Eischeid, and P. J. Pyle, 1994: Interannual variability of the onset of the Indian summer monsoon and its association with atmospheric features, El Niño, and sea surface temperatures. *J. Climate,* **7,** 81–105.

——, K. P. Sooraj, and C. K. Rajan, 2006: The summer monsoon onset over process over south Asia and an objective method for the date of monsoon onset over Kerala. *Int. J. Climatol.,* **26,** 1871–1893.

Kanamitsu, M., W. Ebisuzaki, J. Woollen, S. K. Yang, J. J. Hnilo, M. Fiorion, and G. L. Potter, 2002: NCEP-DOE AMIP-II Reanalysis (R-2). *Bull. Amer. Meteor. Soc.,* **83,** 1631–1643.

Kinuthia, J. H., and G. C. Asnani, 1982: A newly found jet in north Kenya (Turkana channel). *Mon. Wea. Rev.,* **110,** 1722–1728.

Knutson, T. R., and K. M. Weickmann, 1987: 30–60-day atmospheric oscillations: Composite life cycles of convection and circulation anomalies. *Mon. Wea. Rev.,* **115,** 1407–1436.

Koteswaram, P., 1958: The easterly jet stream in the tropics. *Tellus,* **10,** 42–57.

Krishnamurti, T. N., J. Molinari, and H. L. Pan, 1976: Numerical simulation of the Somali jet. *J. Atmos. Sci.,* **33,** 2350–2362.

——, V. Wong, H. L. Pan, R. Pasch, J. Molinari, and P. Ardanuy, 1983: A three-dimensional planetary boundary layer model for the Somali jet. *J. Atmos. Sci.,* **40,** 894–908.

Lavender, S. L., and A. J. Matthews, 2009: Response of the West African monsoon to the Madden–Julian oscillation. *J. Climate,* **22,** 4097–4116.

Lawrence, D. M., and P. J. Webster, 2002: The boreal summer intraseasonal oscillation: Relationship between northward and eastward movement of convection. *J. Atmos. Sci.,* **59,** 1593–1606.

Le Barbé, L., T. Lebel, and D. Tapsoba, 2002: Rainfall variability in West Africa during the years 1950–1990. *J. Climate,* **15,** 187–202.

Li, C., and M. Yanai, 1996: The onset and interannual variability of the Asian summer monsoon in relation to land–sea thermal contrast. *J. Climate,* **9,** 358–375.

LinHo, L. H., X. Huang, and N. Lau, 2008: Winter-to-spring transition in East Asia: A planetary-scale perspective of the South China spring rain onset. *J. Climate,* **21,** 3081–3096.

Louvet, S., B. Fontaine, and P. Roucou, 2003: Active phases and pauses during the installation of the West African monsoon through 5-day CMAP rainfall data (1979–2001). *Geophys. Res. Lett.,* **30,** 2271–2275.

Lumb, F. E., 1966: Synoptic disturbances causing rainy period along the East African coast. *Meteor. Mag.,* **95,** 150–159.

Maloney, E. D., and J. Shaman, 2008: Intraseasonal variability of the West African monsoon and Atlantic ITCZ. *J. Climate,* **21,** 2898–2918.

Matthews, A. J., 2004: Intraseasonal variability over tropical Africa during northern summer. *J. Climate,* **17,** 2427–2440.

Murakami, T., 1987: Effects of the Tibetan Plateau. *Monsoon Meteorology,* C.-P. Chang and T. N. Krishnamurti, Eds., Oxford University Press, 235–270.

——, L.-X. Chen, A. Xie, and M. L. Shresha, 1986: Eastward propagation of 30–60-day perturbations as revealed from outgoing longwave radiation data. *J. Atmos. Sci.,* **43,** 961–971.

Nicholson, S. E., 1996: A review of climate dynamics and climate variability in Eastern Africa. *The Limnology, Climatology and Paleoclimatology of the East African Lakes,* T. C. Johnson and E. O. Odada, Eds. Gordon and Breach, 25–56.

Ogallo, L. J., 1985: Climatology of rainfall in East Africa. *WMO Conf. on GATE, WAMEX and Tropical Meteorology,* Dakar, Senegal, WMO, 96–102.

Okoola, R. E., P. Camberlin, and J. M. Ininda, 2008: Wet periods along the East Africa coast and the extreme wet spell event of October 1997. *J. Kenya Meteor. Soc.,* **2,** 67–83.

Pai, D. S., and R. M. Nair, 2009: Summer monsoon onset over Kerala: New definition and prediction. *J. Earth Syst. Sci.,* **118,** 123–135.

Pohl, B., S. Janicot, B. Fontaine, and R. Marteau, 2009: Implication of the Madden–Julian oscillation in the 40-day variability of the West African monsoon. *J. Climate,* **22,** 3769–3785.

Raju, P. V. S., U. C. Mohanty, and R. Bhatla, 2005: Onset characteristics of the southwest monsoon over India. *Int. J. Climatol.,* **25,** 167–182.

——, ——, and ——, 2007: Interannual variability of onset of the summer monsoon over India and its prediction. *Nat. Hazards,* **42,** 287–300.

Rao, V. B., J. P. Reyes Fernandez, and S. H. Franchito, 2000: Monsoonlike circulations in a zonally averaged numerical model with topography. *Mon. Wea. Rev.,* **128,** 779–794.

Riddle, E. E., and K. H. Cook, 2008: Abrupt rainfall transitions over the Greater Horn of Africa: Observations and regional model simulations. *J. Geophys. Res.,* **113,** D15109, doi:10.1029/2007JD009202.

Rodwell, M. J., 1997: Breaks in the Asian monsoon: The influence of Southern Hemisphere weather systems. *J. Atmos. Sci.,* **54,** 2597–2611.

——, and B. J. Hoskins, 1995: A model of the Asian summer monsoon. Part II: Cross-equatorial flow and PV behavior. *J. Atmos. Sci.,* **52,** 1341–1356.

——, and ——, 1996: Monsoons and the dynamics of deserts. *Quart. J. Roy. Meteor. Soc.,* **122,** 1385–1404.

Slingo, J., H. Spencer, B. Hoskins, P. Berrisford, and E. Black, 2004: The meteorology of the western Indian Ocean and the influence of the East African highlands. *Philos. Trans. Roy. Soc. London,* **363A,** 25–42.

Sultan, B., and S. Janicot, 2000: Abrupt shift of the ITCZ over West Africa and intra-seasonal variability. *Geophys. Res. Lett.,* **27,** 3353–3356.

——, and ——, 2003: The West African monsoon dynamics. Part II: The ''pre-onset'' and the ''onset'' of the summer monsoon. *J. Climate,* **16,** 3407–3427.

Uppala, S. M., and Coauthors, 2005: The ERA-40 Re-Analysis. *Quart. J. Roy. Meteor. Soc.,* **131,** 2961–3012.

Wang, B., Q. Ding, and P. V. Joseph, 2009: Objective definition of the Indian summer monsoon onset. *J. Climate,* **22,** 3303–3316.

Webster, P. J., T. Palmer, M. Yanai, R. Tomas, V. Magana, J. Shukla, and A. Yasunari, 1998: Monsoons: Processes, predictability and the prospects for prediction. *J. Geophys. Res.,* **103,** 14 451–14 510.

Wheeler, M. C., and H. H. Hendon, 2004: An all-season real-time multivariate MJO index: Development of an index for monitoring and prediction. *Mon. Wea. Rev.,* **132,** 1917–1932.

Wu, M. L. C., S. Schubert, and N. E. Huang, 1999: The development of the South Asian summer monsoon and the intraseasonal oscillation. *J. Climate,* **12,** 2054–2075.

Xavier, P. K., C. Marzin, and B. N. Goswami, 2007: An objective definition of the Indian summer monsoon season and a new perspective of the ENSO-monsoon relationship. *Quart. J. Roy. Meteor. Soc.,* **133,** 749–764, doi:10.1002/qj.45.

Xie, P., and P. A. Arkin, 1997: Global precipitation: A 17-year monthly analysis based on gauge observations, satellite estimates, and numerical model outputs. *Bull. Amer. Meteor. Soc.,* **78,** 2539–2558.

Yin, M. T., 1949: A synoptic-aerologic study of the onset of the summer monsoon over India and Burma. *J. Meteor.,* **6,** 393–400.

Yin, X., A. Gruber, and P. Arkin, 2004: Comparison of the GPCP and CMAP merged gauge–satellite monthly precipitation products for the period 1979–2001. *J. Hydrometeor.,* **5,** 1207–1222.

Zorita, E., and F. F. Tilya, 2002: Rainfall variability in northern Tanzania in the March–May season (long rains) and its links to large-scale climate forcing. *Climate Res.,* **20,** 31–40.